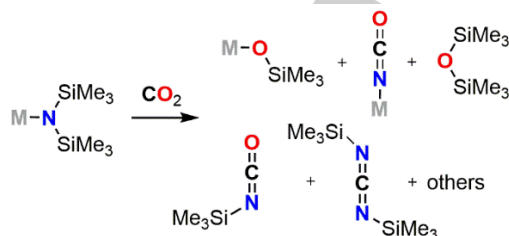# COMMUNICATION

Selective Conversion of CO₂ to Isocyanate by Low–Coordinate Fe

Daniël L. J. Broere,* Brandon Q. Mercado, and Patrick L. Holland*

Abstract: *Discovery of the mechanisms for selective transformations of CO₂ into organic compounds is a challenge. Here, we describe the reaction of low-coordinate Fe silylamide complexes with CO₂ to give trimethylsilyl isocyanate and the corresponding Fe siloxide complex. Kinetic studies show that this is a two-stage reaction, and the presence of a single equivalent of THF influences the rates of both steps. Isolation of a thermally unstable intermediate provides mechanistic insight that explains both the effect of THF in this reaction, and the way in which the reaction achieves high selectivity for isocyanate formation.*

The high abundance, low toxicity and wide availability of CO₂ has sparked great interest towards its use as a C1 building block in organic synthesis.[1] However, the thermodynamic stability of the most oxidized form of carbon poses a challenge for this purpose that is often overcome through the use of highly reactive compounds such as Grignard reagents. Binding of CO₂ to transition metals can lower the activation energy, enabling functionalization using less reactive reagents.[2] The development of efficient methodologies that employ stoichiometric or catalytic amounts of transition metals to utilize CO₂ is greatly aided by fundamental understanding of the underlying reaction mechanisms.[2] This is especially important when reaction products are similar in electronic structure to CO₂, and hence also activated by the metal. A prominent example of such a scenario is the reaction of metal silylamides with CO₂. A wide range of metal silylamides have been reported to react with CO₂ to give isocyanates[3,4,5,6], carbodiimides[7] and metal isocyanato complexes[8] together with the corresponding silyl ethers, metal siloxides or unidentified species (Scheme 1). However, amide additions with high selectivity towards the isocyanate under mild conditions are rare.[4,6] Because the formed isocyanate is isoelectronic with CO₂, metals that strongly activate CO₂ also activate the isocyanate, which is subsequently converted to the carbodiimide or metal isocyanate and silyl ether.


Scheme 1. Common reaction products from the reaction of metal silylamides with CO₂.

Dr. D. L. J. Broere, Dr. B. Q. Mercado, Prof. Dr. P. L. Holland
Department of Chemistry, Yale University
225 Prospect St., New Haven, CT 06511 (USA)
E-mail: daniel.broere@yale.edu / patrick.holland@yale.edu

Supporting information for this article is given via a link at the end of the document xxxxx

We recently reported that Fe[N(SiMe₃)₂]₂[9] gives access to low-coordinate Fe formazanate complex **1** (Scheme 2), and that THF contamination of solvent or starting materials results in the formation of complex **1•THF**.[10] Herein, we show that these complexes both react with CO₂ to selectively give trimethylsilylisocyanate (TMSNCO) and the corresponding siloxide complex, and explain the unusually strong influence of THF through kinetic studies and through the isolation of a key intermediate.

Exposing solutions of either **1** or **1•THF** in non-coordinating solvents to a CO₂ atmosphere (0.9 atm) at room temperature results in the formation of siloxide dimer **2** and 1 equiv of TMSNCO in >95% spectroscopic yield. Removal of volatile components gives a crude product consisting of a 95:5 mixture of **2** and a homoleptic formazanate complex,[11] which is readily washed away to give pure **2**. Compounds **1** and **2** each decompose over several days in benzene solution at ambient temperature to form the homoleptic formazanate complex and other unidentified species, explaining the small amount of homoleptic complex that is formed in the reactions of **1** and **1•THF** with CO₂. The ¹H NMR spectrum of complex **2** in C₆D₆ at 298 K showed the number of paramagnetically shifted resonances between +30 and -16 ppm expected for idealized C_{2v} symmetry (Figure S1). The magnetic moment in C₆D₆ from the Evans method at room temperature was 6.1 ± 0.3 μ_B per dimer, which is lower than the spin-only uncoupled value of 6.9 μ_B and suggests antiferromagnetic coupling between high-spin Fe²⁺ ions (S = 2) in a dimer. The resonances in the ¹H NMR spectrum of complex **2** in THF-d_8 at 298 K are broader and appear at significantly different chemical shifts, indicative of THF coordination that breaks up the dimer to form a monomeric species. However, even in THF solvent a small amount of dimeric **2** is observed at 298 K, which increases in concentration with temperature (Figure S2), consistent with an equilibrium between dimer **2** and a monomeric THF solvate in solution. This is in stark contrast with compound **1**, which fully converted to **1•THF** in the presence of just a single equiv of THF. A van't Hoff analysis (Figure S4) of **2** in THF gave $\Delta H° = -4.3 ± 0.2$ kcal mol⁻¹ and $\Delta S° = -16.9 ± 0.6$ cal mol⁻¹ K⁻¹. The negative reaction entropy is consistent with binding of two THF molecules to form two molecules of monomeric THF-containing complexes. The magnetic moment in THF-d_8 at room temperature from the Evans method is 4.9 ± 0.2 μ_B per monomeric unit, which is consistent with a mononuclear high-spin Fe²⁺ (S = 2) complex.

The zero-field Mössbauer spectrum of a solid sample of **2** at 80 K showed a doublet with δ = 0.84 mm/s and |ΔE_Q| = 1.45 mm/s (Figure S5), consistent with a high spin Fe²⁺ configuration.[12] A frozen THF solution of **2** showed a mixture of two species with comparable isomer shifts (δ = 0.82 and 0.84 mm/s) but different quadrupole splittings (|ΔE_Q| = 1.22 and 0.86 mm/s) (Figure S6). The Mössbauer parameters of one of these signals are similar to those for dimer **2**, in agreement with an equilibrium with a monomeric THF complex that has different Mössbauer parameters.
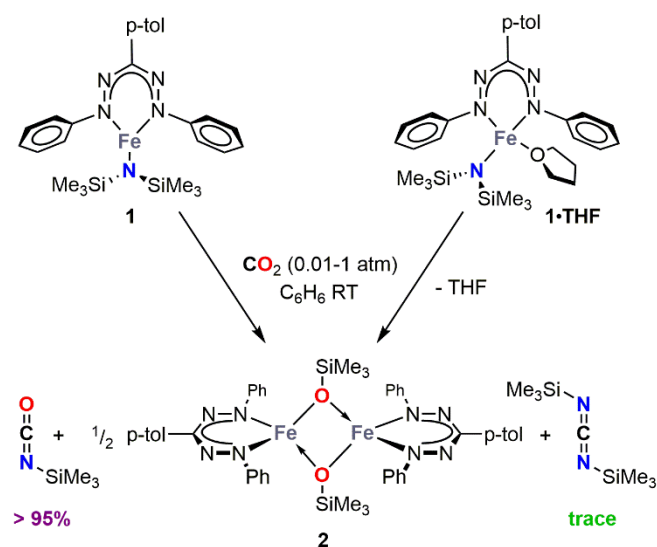
Scheme 2. Reaction of compounds **1** and **1•THF** to form complex **2** and an equiv of TMSNCO.

Crystals of complex **2** grew from a benzene solution at ambient temperature. X-ray crystallographic analysis revealed a dimeric structure where half of the molecule is crystallographically related to the other half by an inversion center (Figure 1). The formazanate–Fe bond lengths (1.978(2) and 1.979(2) Å) are similar to the values for four-coordinate **1•THF** (1.955(4) – 1.966(4) Å). One of the Fe–O bonds is in the same plane as the formazanate ligand, and is significantly shorter than its counterpart (1.954(1) vs 2.056(2) Å), which sticks out of the Fe formazanate plane, similar to the THF ligand in the solid state structure of **1•THF**.[10] The short Fe–Fe distance of 2.9916(5) Å in **2** is conducive to antiferromagnetic coupling of the two high-spin Fe^{2+} centers, described above.
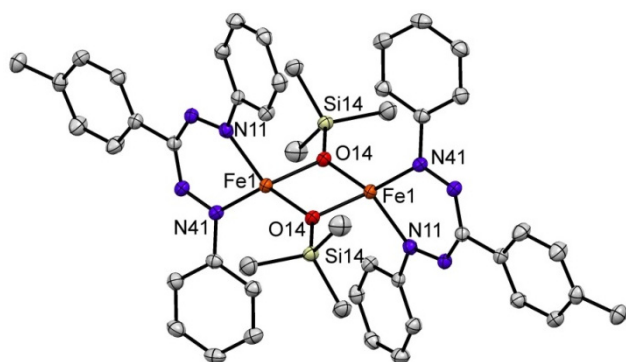

Figure 1. Displacement ellipsoid plots (50% probability) of complex **2**. Hydrogen atoms have been omitted for clarity.

Although reactions of either **1** or **1•THF** with CO_2 give **2** and TMSNCO in high yield, monitoring each reaction by ^1H NMR spectroscopy in C_6D_6 revealed that the two reactions follow distinctly different time courses. In the reaction of **1** with CO_2

(Figure 2, top), rapid consumption of **1** and formation of TMSNCO are observed, but formation of **2** is slower and does not follow an exponential time dependence. Accordingly, there is formation of an intermediate species (**3**) at a similar rate to the disappearance of **1**. After the consumption of **1**, the reaction enters a second stage, and the concentration of intermediate **3** decreases at a similar rates as isocyanate and **2** are formed. These observations indicate a two-stage mechanism starting with rapid conversion of two molecules of **1** to one equiv of TMSNCO and intermediate **3**. The second stage involves a slower decay of **3** into one equiv of **2** and TMSNCO.

In contrast, in the reaction of **1•THF** with CO_2 under identical conditions (Figure 2, bottom), **1•THF** was observed throughout the reaction. Moreover, the rates of formation of **2** and TMSNCO are not as different as in the reaction of THF-free **1** with CO_2. Although intermediate **3** is formed again, along with a short stage with relatively fast formation of TMSNCO, **3** forms in a significantly smaller amount before it goes on to the same products. In addition,
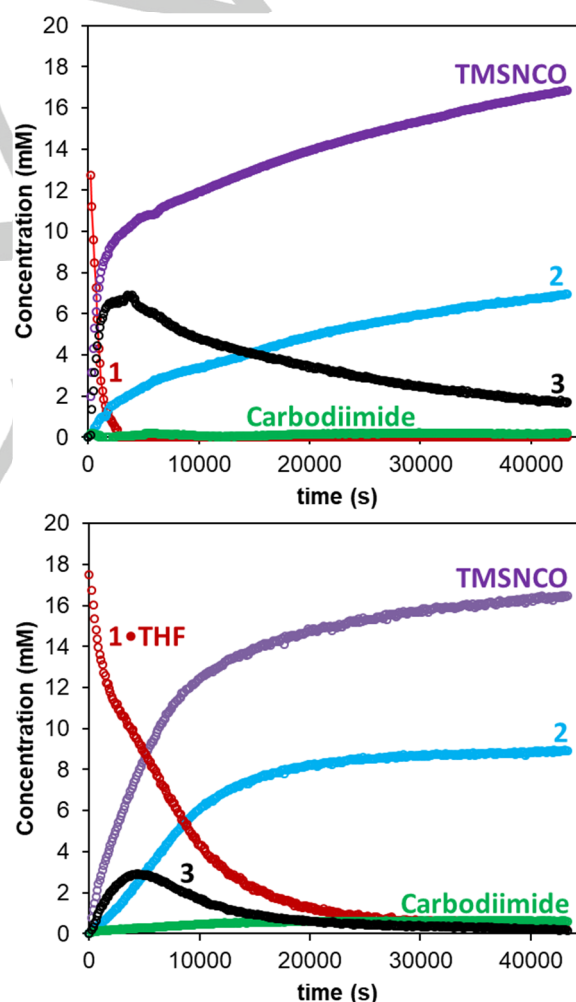
Figure 2. Plots of concentration of starting complex, intermediate and products vs time for the reaction of **1** (top) and **1•THF** (bottom) with CO_2 in C_6D_6.

a small amount (~3%) of bis(trimethylsilyl)carbodiimide is formed in this reaction. Both complexes **1** and **1•THF** reacted with TMSNCO, forming **2** and bis(trimethylsilyl)carbodiimide. We propose that in the reaction of **1•THF** with CO_2 a small amount of carbodiimide is formed because **1•THF** is not rapidly consumed, enabling the side reaction of **1•THF** with formed TMSNCO to give the carbodiimide and **2**. In contrast, the rapid consumption of **1** with CO_2 to give **3** (which does not react with isocyanate) prevents formation of the carbodiimide byproduct.

Intrigued by the marked influence of a single equivalent of THF on the formation and decay of intermediate **3**, we sought to elucidate its structure despite its transient appearance. Performing the reaction of **1** with CO_2 at 0 °C in toluene-d_8 results in full consumption of **1** after 4 h to give **3** in 76% spectroscopic yield with only 23 % of **2**. To discover if an exogenous molecule of CO_2 is required for the conversion of **3** into **2** and TMSNCO, at his stage the solution was submitted to three freeze-pump-thaw cycles to remove all CO_2. Upon warming the solution to room temperature, all **3** quantitatively converts to **2** and TMSNCO, showing that the second equiv of CO_2 is already incorporated in intermediate **3**. Using the poor solubility of **2** to our advantage, we exposed a pentane solution of **1** to CO_2 for 1 h at ambient temperature and placed it at -40 °C for 4 h, resulting in crystallization of all **2**. Concentration of the supernatant and cooling to -40 °C gives crystals of pure **3** in 54% isolated yield. The zero-field Mössbauer spectrum of a solid sample of **3** at 80 K has a doublet with δ = 0.81 mm/s and $|\Delta E_Q|$ = 1.51 mm/s (Figure 3), which are similar to those for solid **2**. The chemical shifts in the ^1H NMR spectrum of the intermediate in C_6D_6 (Figure S8) are in the same range as those of **2**, but all resonances are split into 1:1 pairs, indicating a loss of symmetry. Although two chemically inequivalent formazanate ligands are observed for **3** in C_6D_6 solution, the two corresponding Fe environments in a solid sample of **3** are indistinguishable by Mössbauer spectroscopy, suggesting that they have similar geometries. The ^1H NMR spectrum of **3**, and the observation that two equivalents of **1** are consumed to produce one equivalent of **3**, which quantitatively decays to give a single molecule of dimeric **2**, suggests that **3** has a nonsymmetrical dimeric structure.

The isolation of **3** also enabled us to test its reactivity. Notably, the rate of the conversion of **3** into **2** and TMSNCO is much more rapid in the presence of THF (Figure S10), explaining the lower buildup and faster decay of **3** in the reaction of **1•THF** with CO_2. The IR spectrum of **3** shows two bands at 1351 and 1514 cm^{-1} that are not observed in the IR spectra of **1**, **1•THF**, or **2** (Figure S9). The infrared spectrum of a sample of **3** that was prepared using isotopically labeled $^{13}CO_2$ gas (Figure S11) had these bands shifted to 1321 and 1468 cm^{-1}, respectively. These values are in the expected range for the C–N and C–O stretching frequency of a metal bound *N*-substituted carbamate anion.[13] Uncoordinated *N*-substituted carbamate ester anions in solution have been observed to convert into the respective isocyanate and alkoxide,[14] in agreement with the observed reactivity of **3**.

Crystals suitable for X–ray diffraction were obtained by cooling a solution of **3** in pentane to -40 °C. The solid state structure (Figure 4) revealed a nonsymmetric dinuclear complex with a bridging alkoxide and *N*-substituted carbamate anion, in agreement with the IR and ^1H NMR spectra.
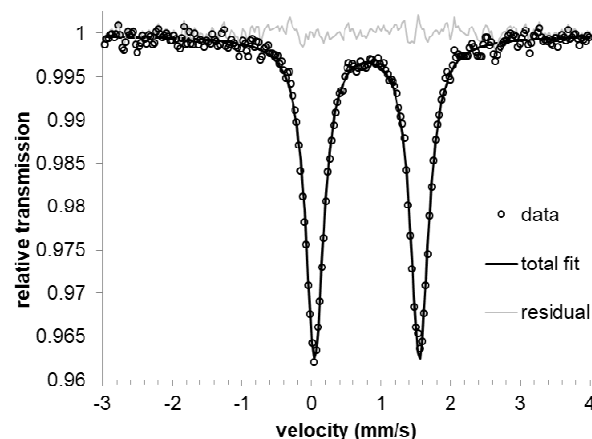
Figure 3. Zero-field Mössbauer spectrum of a solid sample of complex **3** at 80 K. δ = 0.81 mm/s and $|\Delta E_Q|$ = 1.51 mm/s.

Two crystallographically independent molecules are found in the asymmetric unit that differ in the relative orientation of the two formazanate ligands in the dinuclear complex (Figure S12). The two independent molecules have very similar bond lengths and angles around the Fe centers. Within the central six-membered ferracycle the Fe1–O17 and Fe1–O18 distances are ~0.08 Å longer than the Fe2–N17 and Fe2–O18. Similarly, the O18–Fe1–O17 angle of 97.6(1)° is significantly smaller than the O18–Fe2–N17 angle of 113.4(1)°. The difference electron density map did not allow unambiguous assignment of O and N atoms within the bridging carbamate ligand. Fortunately, the bond lengths within the carbamate do show clear differences that enable this distinction. The bonds to C17 show clear partial double bond character for the O17–C17 (1.266(3) Å) and N17–C17 (1.313(3) Å) bonds. The longer O27–C17 distance of 1.348(3) Å is in the expected range for a C–OSiMe$_3$ single bond.[15] A CCSD search of O–SiMe$_3$ and N–SiMe$_3$ bonds where O or N is also bound to Fe showed that these are between 1.599–1.709 Å and 1.690–1.802 Å with mean values of 1.650 Å and 1.733 Å, respectively. The N17–Si27 bond distance of 1.776(2) Å is outside of the range for
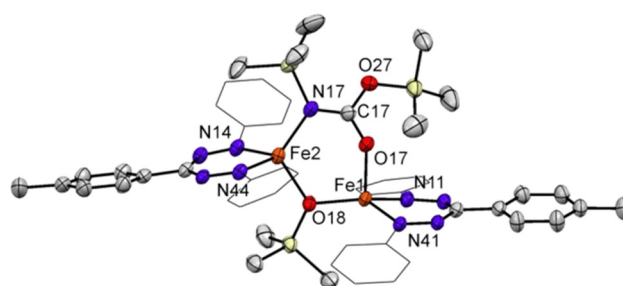
Figure 4. Displacement ellipsoid plot (50% probability) of complex **3**. Hydrogen atoms have been omitted for clarity. Selected bond lengths (Å) and angles (°) Fe1–O18 1.957(1); Fe1–O17 1.974(2); Fe1–N11 1.987(2); Fe1–N41 1.989(2); Fe2–N14 1.967(2); Fe2–N44 1.978(2); Fe2–N17 2.023(2); Fe2–O18 2.034(15); O18–Fe1–O17 97.59(6); N11–Fe1–N41 90.13(8); N14–Fe2–N44 90.42(8); N17–Fe2–O18 113.39(7).

reported O–Si bonds. In addition, it is significantly longer than the Si17–O27 bond distance (1.686(2)), which is comparable to the O–Si bond distances of O18 in **3** (1.660(2) Å) and O14 in **2** (1.649(1) Å), and within the range of O–Si bonds in the CCSD. A different CCSD search revealed only a few examples of *N*-substituted carbamate esters that bridge two metals.[16] The bond lengths within the bridging *N*-substituted carbamate ester in **3** are comparable to these examples.[13a,16] Notably, in most examples[17] these were formed by reaction of an alkoxide ligand with isocyanates, which is also the case for *N*-substituted carbamate esters that are bound to a single metal center[18]. Interestingly, complex **3** displays the opposite reaction, and **2** does not react with excess TMSNCO.

Scheme 3 shows a mechanism that explains the difference in reactivity between **1** and **1•THF** with CO_2, and is in agreement with the experimental data. In this mechanism, coordination of CO_2 occurs to THF-free **1** and not to the THF-bound **1•THF**, and thus **1•THF** reacts more slowly with CO_2 than **1** because it is strongly inhibited by THF. Moreover, this THF inhibition indicates that CO_2 coordination to iron is necessary for the reaction to proceed. Attack of the silylamide on coordinated CO_2, followed by migration of the SiMe3 group, gives **B** which rapidly reacts to form **3** and ½ equiv TMSNCO. Both the formation of **2** from **3**, and loss of isocyanate from **B**, are more rapid in the presence of THF through formation of **D**, which rapidly converts to **2**. This mechanistic model explains the faster decay and lower buildup of **3** in the reaction of **1•THF** with CO_2 compared to its THF-free counterpart.
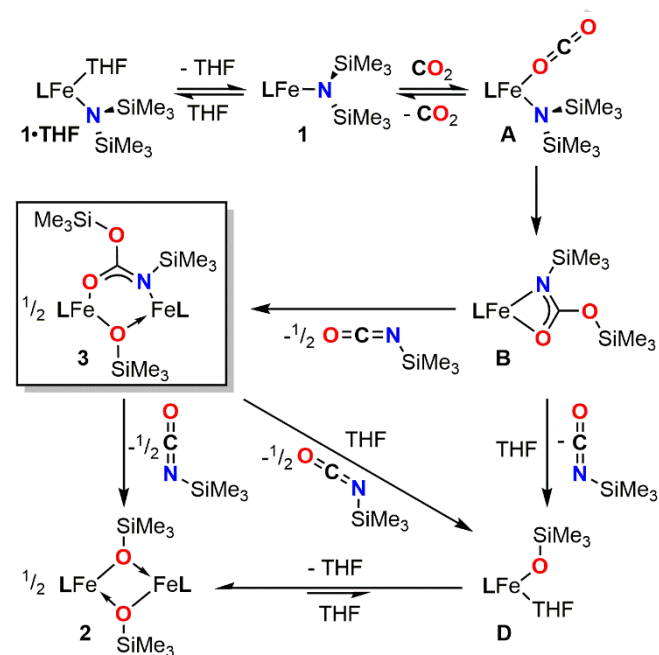
complex. The presence of a single equiv of THF slows the progress toward a key carbamate intermediate, and increases the rate of the intermediate's conversion to products. The results here give kinetic evidence for the importance of CO_2 coordination during its activation, and also show how relative rates can be manipulated to achieve high selectivity.

Acknowledgements

[1] a) J. Klankermayer, S. Wesselbaum, K. Beydoun, W. Leitner, *Angew. Chem. Int. Ed.* **2016**, *55*, 7296–7343; b) M. Aresta, A. Dibenedetto, A. Angelini, *Chem. Rev.* **2014**, *114*, 1709–1742; c) T. Sakakura, J. –C. Choi, H. Yasuda, *Chem. Rev.* **2007**, *107*, 2365–2387; d) M. Aresta, in *Carbon Dioxide as Chemical Feedstock* (Eds.: M. Aresta), Wiley–VCH, Weinheim, **2010**, pp. 1-13.

[2] Q. Liu, L. Wu, R. Jackstell, M. Beller, *Nat. Commun.* **2015**, *6*, 5933–5948.

[3] a) M. Reiter, S. Vagin, A. Kronast, C. Jandl, B. Rieger, *Chem. Sci.* **2017**, *8*, 1876–1882; b) D. R. Moore, M. Cheng, E. B. Lobkovsky, G. W. Coates, *J. Am. Chem. Soc.* **2003**, *125*, 11911–11924.

[4] D. A. Dicki, K. B. Gislason, R. A. Kemp, *Inorg. Chem.* **2012**, *51*, 1162–1169.

[5] H. Yin, P. J. Carroll, E. J. Schelter, *Chem. Commun.* **2016**, *52*, 9813–9816.

[6] A. M. Felix, B. J. Boro, D. A. Dickie, Y. Tang, J. A. Saria, B. Moasser, C. A. Stewart, B. J. Frost, R. A. Kemp, *Main Group Chem.* **2012**, *11*, 13–29.

[7] L. R. Sita, J. R. Babcock, R. Xi, *J. Am. Chem. Soc.* **1996**, *118*, 10912–10913.

[8] a) C. Camp, L. Chatelain, C. E. Kefalidis, J. Pécaut, L. Maron, M. Mazzanti, *Chem. Commun.* **2015**, *51*, 15454–15457; b) M. T. Whited, A. J. Kosanovich, D. E. Janzen, *Organometallics* **2014**, *33*, 1416–1422; c) P. Arnold, Z. R. Turner, A. I. Germeroth, I. J. Casely, G. S. Nichol, R. Bellabarba, R. P. Tooze, *Dalton Trans.* **2013**, *42*, 1333–1337; d) W. Sattler, G. Parkin, *J. Am. Chem. Soc.* **2011**, *133*, 9708–9711; e) B. C> Fullmer, H. Fan, M. Pink, K. G. Caulton, *Inorg. Chem.* **2008**, *47*, 1865–1867; f) H. Phull, D. Alberti, A. L. Korobkov, S. Gambarotta, P. H. M. Budzelaar, *Angew. Chem. Int. Ed.* **2006**, *45*, 5331–5334.

[9] a) D. L. J. Broere, I. Čorić, A. Brosnahan, P. L. Holland, *Inorg. Chem.* **2017**, *56*, 3140–3143; b) M. M. Olmstead, P. P. Power, S. Shoner, *Inorg. Chem.* **1991**, *30*, 2547–2551; c) R. A. Andersen, K. Faegri, J. C. Green, A. Haaland, M. F. Lappert, W. Leung, K. Rypdal, *Inorg. Chem.* **1988**, *27*, 1782–1786.

[10] D. L. J. Broere, B. Q. Mercado, J. T. Lukens, A. C. Vilbert, G. Banerjee, H. M. C. Lant, S. H. Lee, E. Bill, S. Sproules, K. M. Lancaster, P. L. Holland, submitted.

[11] R. Travieso-Puente, J. O. P. Broekman, M. –C. Chang, S. Demeshko, F. Meyer, E. Otten, *J. Am. Chem. Soc.* **2016**, *138*, 5503–5506.

[12] S. F. McWilliams, E. Brennan–Wydra, K. C. MacLeod, P. L. Holland, *ACS Omega* **2017**, *2*, 2594−2606.

[13] a) A. Garci, A. A. Dobrov, T. Riedel, E. Orhan, P. J. Dyson, V. B. Arion, B. Therrien, *Organometallics* **2014**, *33*, 3813–3822; b) A. K. Mishra, R. N. Singh, A. K. Chaturvedi, K. K. Singh, *Int. J. Chem. Sci.* **2014**, *12*, 1289–1298; c) C. Köthe; R. Metzinger, C. Limberg, C. *Eur. J. Inorg. Chem.* **2013**, 3937–3942; d) G. N. Andreev, J. Petrov, V. Ognyanova, *Spectrosc. Lett.* **1997**, *30*, 717–726; e) J. G. Noltes, J. Boersma, *J. Organometal. Chem.* **1969**, *16*, 345–355.

Scheme 3. Proposed mechanism for the conversion of CO_2 into TMSNCO with and without THF.

In conclusion, we have shown that low-coordinate Fe silylamide complexes bearing formazanate ligands react with CO_2 to selectively give TMSNCO and the corresponding Fe siloxide

[14]   a) A. F. Hegarty, L. N. Frost, *J. Chem. Soc., Chem. Commun.* **1972**, *0*, 500–501; b) D. J. Woodcock, *Chem. Commun.* **1968**, *0*, 267–269.

[15]   H. –W. Lerner, M. Bolte, M. Wagner, *Dalton Trans.* **2017**, *46*, 8769–8773.

[16]   a) M. H. Chisholm, F. A. Cotton, K. Folting, J. C. Huffman, A. L. Ratermann, E. S. Shamshoum, *Inorg. Chem.* **1984**, *23*, 4423–2227; b) F. A. Cotton, E. S. Shamshoum, *J. Am. Chem. Soc.* **1985**, *107*, 4662–4667; c) M. C. Barral, S. Herrero, R. Jiménez–Aparicio, J. L. Priego, M. T. Torres, F. A. Urbanos, *J. Mol. Struct.* **2008**, *890*, 221–226; d) H. –Q. Do, S. Bachman, A. C. Bissember, J. C. Peters, G. C. Fu, *J. Am. Chem. Soc.* **2014**, *136*, 2162–2167; e) S. Roy, B. Sarkar, H. –G. Imrich, J. Fiedler, S. Záliš; R. Jimenez–Aparicio, F. A. Urbanos, S. M. Mobin, G. Lahiri, W. Kaim, *Inorg. Chem.* **2012**, *51*, 9273–9281; f) V. Körner, S. Vogel, G. Huttner, L. Zsolnai, O. Walter, *Chem. Ber.* **1996**, *129*, 1107–1113.

[17]   We exclude the examples that have the same carbamate binding motif from coordination of a deprotonated 2–oxazolidinone or hydrazine.[16d–f] A single example was found that involves a reaction of CO_2 with a benzamidinato ligand to give a thermally stable ligand-derived carbamate on Ni: D. Walther, P. Gebhardt, R. Fischer, U. Kreher, H. Görls, *Inorg. Chim. Acta.* **1998**, *281*, 181–189.

[18]   a) R. Pothiraja, A. P. Milanov, D. Barreca, A. Gasparotto, H. –W. Becker, M. Winter, R. A. Fischer, A. Devi, *Chem. Commun.* **2009**, *0*, 1978–1980; b) R. Ghosh, M. Nethaji, A. G. Samuelson, *J. Organomet. Chem.* **2005**, *690*, 1282–1293; c) M. A. Lockwood, P. E. Fanwick. I. P. Rothwell, *Organometallics* **1997,** *16,* 3574–3575; d) V. C. Gibson, C. Redshaw, W. Clegg, M. R. J. Elsegood, *J. Chem. Soc., Chem. Commun.* **1994**, 2635–2636.